Journal of Nuclear Materials 386–388 (2009) 422–425

Contents lists available at ScienceDirect

Journal of Nuclear Materials

journal homepage: www.elsevier.com/locate/jnucmat

Effect of helium on tensile properties and microstructure in 9%Cr–WVTa–steel after neutron irradiation up to 15 dpa between 250 and 450 °C

E. Materna-Morris [a,*], A. Möslang [a], R. Rolli [b], H.-C. Schneider [b]

[a] Forschungszentrum Karlsruhe, Institut für Materialforschung I, P.O. Box 3640, 76021 Karlsruhe, Germany
[b] Forschungszentrum Karlsruhe, Institut für Materialforschung II-FML, P.O. Box 3640, 76021 Karlsruhe, Germany

A B S T R A C T

Helium formation in reduced-activation martensitic-ferritic (RAFM) 8–10%Cr–WTaV steels and their impact on mechanical properties are primary subjects of fusion materials research. In this connection, three heats were melted with different ^{nat}B- and ^{10}B-contents on the basis of the chemical composition of EUROFER97. EUROFER97 had the lowest content of ^{nat}B < 10 ppm. Two heats were alloyed with boron, one with ~82 ppm ^{nat}B and the other with ~83 ppm ^{10}B, and a third heat with a very high concentration of ~1160 ppm ^{10}B. Tensile specimens were irradiated up to ~15 dpa at 250–450 °C. The post-irradiation tensile tests showed the typical strengthening between 250 and 350 °C. The effect of the dpa and irradiation temperature was explained by microstructural changes, such as dislocation loops, α′-precipitates, and helium bubbles. The lower ^{10}B containing specimens exhibited a ductile fracture appearance, but with a loss in elongation. The specimens with the highest concentration of ^{10}B exhibited always a brittle fracture appearance. The phenomena observed in the microstructures and fractures were correlated with the mechanical properties.

1. Introduction

8–10%Cr–WTaV steels are a successful material for the use in a wide temperature range [1–5]. Such advanced martensitic steels are leading candidates for fusion structural components. They are interesting due to their resistance to void swelling, and good balance of different physical and mechanical properties. However, a critical effect of low temperature irradiation induced hardening and embrittlement occurs in the range of 250–350 °C. One reason was found in the radiation induced microstructural changes in the material, especially the production of He. While in fission reactors without B or Ni doping the He to displacement damage ratio is typically 0.1–0.3 appm He/dpa it amounts to ~10 appm He/dpa in a first wall of a fusion reactor. In a recent past results of accelerator He implantations have shown the importance of He effects on microstructure [6–8].

The objective of the present paper is to characterize a series of martensitic test alloys with various ^{10}B- and ^{nat}B-doping to investigate systematically the influence of neutron irradiation generated He on tensile properties and microstructure. The irradiation was performed up to an accumulated dose of ~15 dpa in the HFR (High Flux Reactor, Petten, Netherlands). The achieved He concentration by ^{10}B(n,α)^{7}Li generation was <10 appm He, ~80 appm He, ~415 appm He, and ~5800 appm He, respectively. Initial results of tensile tests, SEM (scanning electron microscopy) and TEM (transmission electron microscopy) are reported in this study.

2. Experimental procedure

Three alloys on the bases of the RAFM-steel EUROFER97 were melted in 25 kg-heat each with different ^{10}B- and ^{nat}B-contents and compared with EUROFER97 reference heat (7 tons). The chemical compositions of these test alloys were defined in Forschungszentrum Karlsruhe, Institut für Materialforschung I, and ordered at the steel producer SAARSTAHL, Table 1. The material was delivered in 25 × 25 mm square bar steels. Austenitization and annealing behaviour were determined. The optimized heat treatment was the same in all alloys: 1040 °C 30 min + 760 °C 90 min.

Circular tensile specimens were fabricated with a total length of 38 mm, and a gauge length of 18 mm and 3 mm diameter. They were taken parallel to the rolling direction. A special wrapper, with irradiation capsules accommodating the tensile- and further impact and fatigue specimens, was inserted in the central part of the reactor core of HFR. The irradiation was set to 250, 300, 350, 400, and 450 °C. Temperatures were controlled by changing the gas mixture (helium and neon) in the gas gaps surrounding the samples. The cumulative neutron fluence $E > 0.1$ MeV m^{-2} was 22.85×10^{25}. The neutron irradiation was carried out in 771 FPD (full power days) up to nominal dose of ~15 dpa. The experimental obtained damage levels for monitor set positions in the specimens holder varied between 13.4 and 18.1 dpa. Neutronic calculations

* Corresponding author. Tel.: +49 7247 82 2162; fax: +49 7247 82 4567.
E-mail address: materna-morris@imf.fzk.de (E. Materna-Morris).

0022-3115/$ - see front matter © 2009 Elsevier B.V. All rights reserved.
doi:10.1016/j.jnucmat.2008.12.157

Table 1
Chemical compositions of the test alloys.

Heat	C	Si	Mn	P	S	Cr	Mo	Ni	Al
EUROFER97	0.12	0.04	0.48	0.005	0.004	8.91	<0.001	0.02	0.009
806	0.109	0.020	0.602	0.0035	0.0030	9.31	0.002	0.005	0.001
826	0.095	0.031	0.395	0.0035	0.003	8.80	0.046	0.008	0.004
825	0.10	0.03	0.38	0.001	0.0025	9.00	0.028	0.006	0.004

	B	Nb	Ti	V	W	N	Ta	Fe
EUROFER97	<0.001 ^{nat}B	0.0017	0.001	0.2	1.08	0.02	0.14	Rest
806	0.0082 ^{nat}B	–	–	0.190	1.27	0.021	0.055	Rest
826	0.0083 ^{10}B	0.005	0.001	0.193	1.125	0.028	0.088	Rest
825	0.1160 ^{10}B	0.002	0.001	0.197	1.06	0.0255	0.08	Rest

have shown that the volume-average displacement dose of all specimens was 16.3 dpa for stainless steel. The irradiation project was named HFR Phase-IIb (SPICE).

After the irradiation, the specimens were transported to the hot cells of the FML (Fusion Material Laboratories) Forschungszentrum Karlsruhe to perform the tensile tests. All tests were carried by instrumented tensile testing machine with a tensile velocity of 0.1 mm/min. Test temperatures were the same as the irradiation temperatures. The un-irradiated specimens were tested at 20, 300 and 450 °C to determine the thermal and irradiation induced influence.

Fractures and the microstructures were investigated by light and electron microcopy at specimens of the highest ultimate strength at 300 °C and the highest irradiation temperature of 450 °C. TEM (transmission electron microscopy) specimens were cut transverse from the gauge length of the tensile specimens. This material was deformed by tensile testing, and it was compared with un-deformed material of impact tests [9,10]. Material segregations and inclusions of B were controlled by Auger-analysis. Hardness was measured by Vickers HV0.1.

3. Results and discussion

3.1. Tensile properties

After the irradiation, the tensile tests were recorded fully instrumented in stress/strain diagrams. Every material condition was irradiated and tested by two specimens. In Figs. 1–3 all the tensile results of EUROFER97, heat 806 and 826 are shown. EUROFER97, heat 806 and 826 had the highest strength at 300 °C. At higher irradiation and test temperatures up to 450 °C, the data

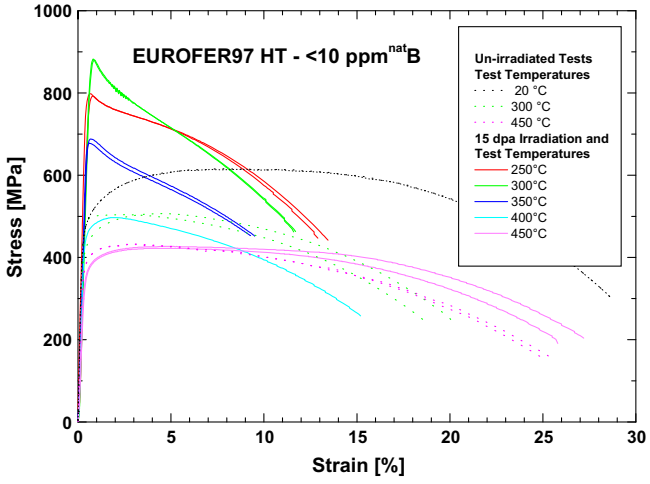

Fig. 1. Tensile properties of EUROFER97.

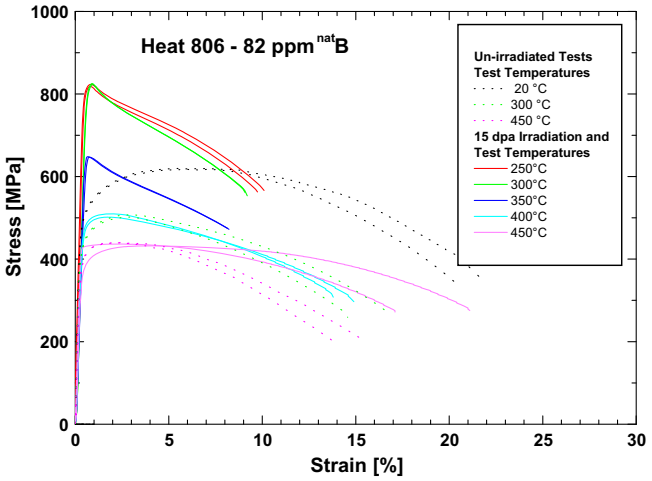

Fig. 2. Tensile properties of heat 806.

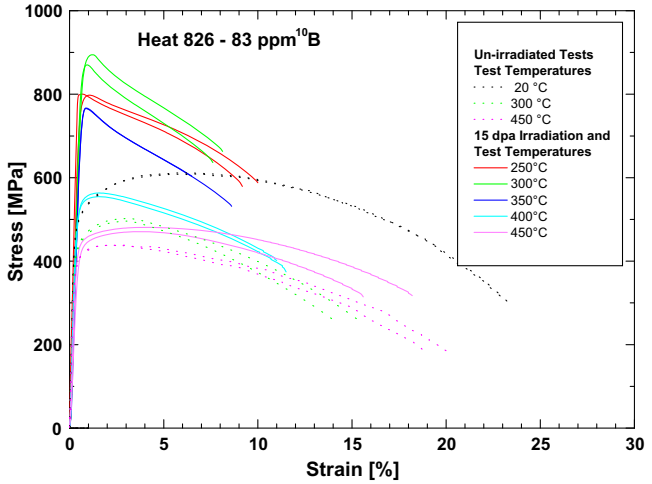

Fig. 3. Tensile properties of heat 826.

reached the level of un-irradiated materials, but still with a reduction in elongation, due to the limitation of the thermal stability of interstitial type defects and small precipitates. The strength of heat 826 (83 ppm ^{10}B; ~415 appm He) was systematically higher than of heat 806 (82 ppm ^{nat}B; ~80 appm He). As in the ^{10}B doped alloy all B is transmuted to He after 1 dpa has been reached. The additional induced strength increase of heat 826 compared to heat 806 can be interpreted as a direct proof, how He contributes to irradiation induced hardening at different irradiation temperatures. The absolute strength values of EUROFER97 can only be compared in a relative manner to these test heats, because it has

been produced as a large batch. The third test heat 825 (1160 ppm ^{10}B; ~5800 appm He) had a similar strength behaviour, but, at lower temperatures, the specimens had a brittle fracture after having reached stress levels of 700–850 MPa.

3.2. Hardness and fracture behaviour

He dependence could be seen in the comparison of heat 806 and 826; the ^{10}B containing alloy 826 had always higher strength than the ^{nat}B-containing heat 806. This strengthening could be approved in hardness measurements, too. The higher concentration of He bubbles caused a ~10% higher hardness resulting in a higher strength.

EUROFER97, heat 806, and 826 exhibited always a ductile fracture with typical dimple formations. In heat 826, small brittle areas could be found around former B-precipitates Fig. 4. This effect is irradiation induced, and could be observed much more in heat 825. These fractures occurred much more brittle, mainly at grain boundaries.

3.3. Microstructural evolution

Before irradiation, the distribution of the alloyed boron was controlled in the structure of the heats. In heat 806 and 826 some B inclusion could be analyzed. Much more B inclusions and further precipitates as (Cr,Fe)B and B(C,N) were found in heat 825. In heat EUROFER97, just few inclusions of MnS and oxides were detected. TaC and $M_{23}C_6$ were dominant in all heats. Prior austenitic grain sizes of ASTM 6–7 were determined in the metallographic cuts. Heat 826 showed a tendency to coarser grain due to the lower content of the primary carbide forming element Ta.

Microstructures of the heats were investigated in TEM in the un-irradiated and irradiated state after 250, 300 and 450 °C. At the lower irradiation temperature, the microstructure was characterized by dislocation loops and α′-precipitates. Only very few areas with dislocation channeling were observed at 300 °C after tensile test. In EUROFER97 only few individual He bubbles were detected in the matrix, while in heat 806 small clusters of He bubbles have been observed. In contrast to EUROFER97 and heat 806, an almost homogenous distribution of He bubbles was shown up in heat 826. As expected, in all heats the He bubbles size increases with irradiation temperature. The presented pictures are from the un-deformed materials, Figs. 5–8. Fig. 9 shows an example of tensile tested microstructure of EUROFER97. The dislocation loops were oriented with a trend to form alignments to the gliding directions of the bcc crystal structure.

The microstructure of heat 825 was especially noticeable, Fig. 8. After the irradiation at 300 °C, a homogenous distribution of bubbles could be seen in the matrix, but, after 400 °C irradiation, there was a bi-modal distribution of bubbles.

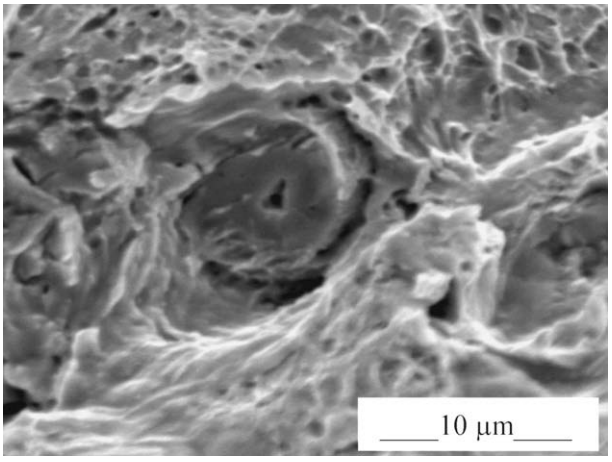

Fig. 4. Fracture area around a former B-precipitate in heat 826, irradiated and tensile tested at 300 °C.

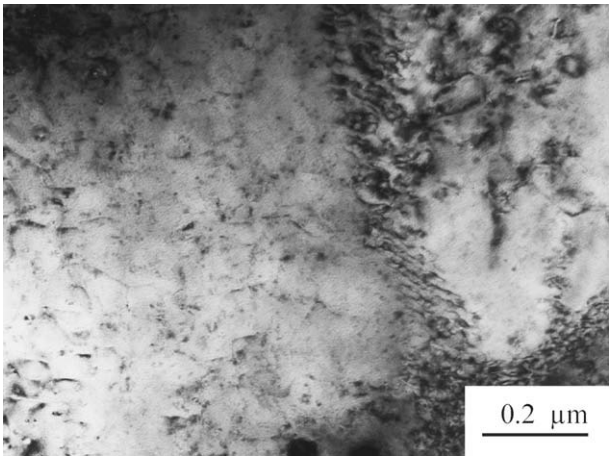

Fig. 5. Microstructure of EUROFER97 HT (<10 appm He); irradiated at 250 °C.

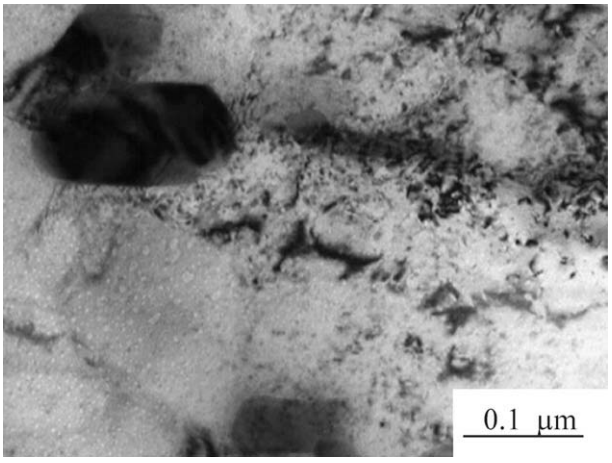

Fig. 6. Microstructure of heat 806 (~80 appm He); irradiated at 250 °C.

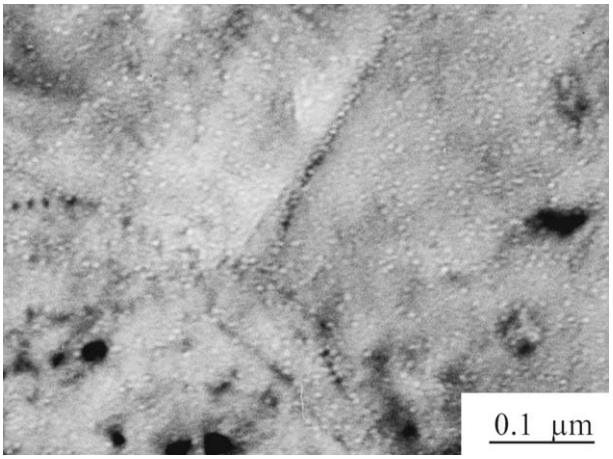

Fig. 7. Microstructure of heat 826 (~415 appm He); irradiated at 250 °C.

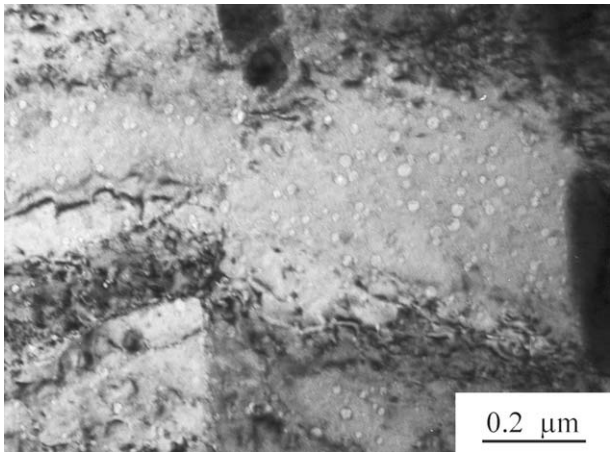

Fig. 8. Microstructure of heat 825 (~5800 appm He); irradiated at 300 °C.

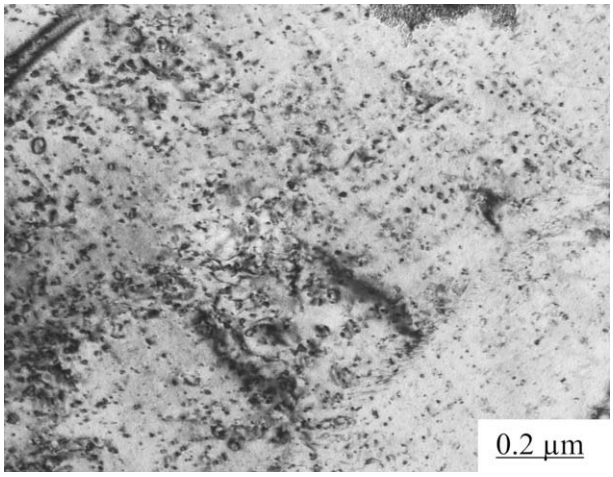

Fig. 9. Microstructure of EUROFER97 HT (<10 appm He); irradiated and tensile tested at 300 °C.

Much more detailed analysis of tensile fracture and TEM results will be published in a forth coming paper.

4. Conclusions

- The expected strengthening at lower temperatures at 250–300 °C irradiation and test temperature were confirmed.
- The hardening and strengthening in the test alloys were generated by dislocation loops, α′-precipitates, and to a less extend be He.
- After tensile tests of 300 °C, a trend to form alignments of dislocation loops have been observed with a typical line distance of ~20 nm.
- Heats with the same B contents, one with ^{nat}B and the other with ^{10}B alloyed, showed the clear difference irradiation induced strengthening due to the generated different He concentrations.
- The thermally induced recovery and the hardening effect of dislocation loops and α′-precipitates was dissolved, which was observed by TEM in specimens of irradiation temperature >400 °C.

Acknowledgements

This work, supported by the European Communities under the contract of Association between EURATOM and Forschungszentrum Karlsruhe, was carried out within the framework of the European Fusion Development Agreement.

References

[1] K. Ehrlich, Philos. Trans. R. Soc. London, A 357 (1999) 595.
[2] K. Ehrlich, D.R. Harries, A. Möslang, Characterization and Assessment of Ferritic/Martensitic Steels, Report FZKA 5626, February 1997.
[3] E. Materna-Morris, M. Rieth, K. Ehrlich, Effects of Radiation on Materials: 19th International Symposium, ASTM STP1366, March 2000, p. 597.
[4] R.L. Klueh, D.R. Harries, 'High-Chromium Ferritic and Martensitic Steels for Nuclear Applications', ASTM Stock Number: MONO3, ISBN 0-8031-2090-7, 2001.
[5] N. Baluc, D.S. Gelles, S. Jitsukawa, A. Kimura, R.L. Klueh, G.R. Odette, B. van der Schaaf, Jinnan Yu, J. Nucl. Mater. 367–370 (2007) 33.
[6] E. Materna-Morris, H.-C. Schneider, B. Dafferner, R. Rolli, O. Romer, A. Möslang, Proceedings of the 20th IEEE/NPSS Symposium on Fusion Engineering, October 14–17, 2003, San Diego, CA USA, 246.
[7] R.J. Kurtz, G.R. Odette, T. Yamamoto, D.S. Gelles, P. Miao, B.M. Oliver, J. Nucl. Mater. 367–370 (2007) 417.
[8] H. Ogiwara, A. Kohyama, H. Tanigawa, H. Sakasegawa, J. Nucl. Mater. 367–370 (2007) 428.
[9] E. Gaganidze, H.-C. Schneider, B. Dafferner, J. Aktaa, J. Nucl. Mater. 367–370 (2007) 81.
[10] E. Gaganidze, C. Petersen, J. Aktaa, 'Helium Embrittlement of RAFM Steels', Poster, ICFRM-13, Nice, December 10–14, 2007.